



Onset and departure of flow boiling heat transfer characteristics of cyclohexane in a horizontal minichannel



Zhaohui Liu, Qincheng Bi*

State Key Laboratory of Multiphase Flow in Power Engineering, Xi'an Jiaotong University, Xi'an 710049, PR China

ARTICLE INFO

Article history:

Received 3 March 2015

Received in revised form 20 April 2015

Accepted 24 April 2015

Keywords:

ONB

Nucleation hysteresis

Flow boiling

Heat transfer deterioration

Cyclohexane

ABSTRACT

The flow boiling behavior of cyclohexane was experimentally investigated in a horizontal minichannel with inner diameter of 2.0 mm. The nucleation hysteresis phenomena at onset of nucleate boiling (ONB) and characteristics at departure of flow boiling were focused on. Both the temperature overshoot due to nucleation hysteresis and wall superheat to maintain boiling conditions decreased with the increasing pressure. The nucleation hysteresis can be clearly observed at pressure of (1.0 and 2.0) MPa, but disappeared at 3.0 MPa. A wall temperature decrease phenomenon (TDP) was found to occur just before flow boiling heat transfer deterioration (HTD). The magnitudes of TDP would be less than 10 °C, but bigger than the temperature overshoot of about 3 °C at ONB. Wherever HTD happened at the saturation boiling conditions with high or low vapor quality ranging from 0 to 1, the TDP were observed, but suppressed by the increasing pressure. Accordant with nucleate hysteresis, the TDP were clearly recorded at $P = 1.0$ and 2.0 MPa, but disappeared at 3.0 MPa. The mechanism of TDP before HTD at flow boiling condition, a problem needed extensive focus investigation, may give a better understanding or even a universe CHF mechanism for both dryout and burnout conditions.

© 2015 Elsevier Ltd. All rights reserved.

1. Introduction

The flow boiling heat transfer in mini/micro channel has been focused and widely researched in the last two decades [1–8]. The important processes and engineering issues including flow distribution, flow instability, nucleation processes, boiling heat transfer and pressure drop were reviewed by Bergles et al. [2] when channel diameters decrease for the design of practical systems. Kandlikar [3–6] investigated and reviewed fundamental issues of flow boiling and heat transfer mechanism in mini/micro channels. The criteria to recognize and differentiate the onset of subcooled boiling, partial boiling, fully developed boiling, and significant void flow were recommended and validated [3]. The effect of surface tension on flow pattern, flow instability and pressure drop fluctuations were discussed in the small diameter channel heat exchanger [4]. As the channel diameter became smaller, larger wall superheat were required for nucleation in microchannels [5]. Correlations to predict heat transfer coefficients for laminar flow, transition flow, and low laminar flow ($150 < Re_{LO} < 450$) and deep laminar flow ($Re_{LO} \leq 100$) were recommended or proposed for mini/micro channels [6]. Kim and Mudawar [7,8] conclusively reported saturation flow boiling performance in mini/micro

channels for 18 working fluids, and proposed generalized correlations to predict dryout incipience qualities, two phase heat transfer coefficient in nucleate boiling dominated and convective boiling dominated heat transfer regimes.

The mini/micro channels are widely used as heat sinks [1] in aerospace flight, electrical cooling, and so on. The space and/or weight constraints in the small scale devices make the cooling channel much tinier, and also the small passages may provide a high performance. In applications for which the coolant enters the channel in the subcooling condition, the designer of the heat exchanger expects that the subcooled boiling occurs in the earliest point of the channel without drying out or departure of nucleate boiling (DNB) in the end of the channel. The flow boiling heat transfer processes are usually used in the high heat flux removal applications [2]. However, the underlying mechanism of the flow boiling, especially the subcooled flow boiling in mini/micro channel are still an open question.

As well known that at the beginning of flow boiling process at start-up, it requires a higher degree of wall superheat to nucleate the bubble [3]. Once the boiling is initiated, the required superheat to sustain the bubble activity is lower. This behavior is known as the hysteresis effect, which is significant in highly wetting liquids such as refrigerants. Lie and Lin [9] found a significant wall temperature overshoot of approximately 20 °C at onset of nucleate

* Corresponding author.

Nomenclature

D	internal diameter (m)
G	mass velocity ($\text{kg/m}^2 \text{ s}$)
h	enthalpy (J/kg)
I	electrical current (A)
L	heated length (m)
M	mass flow rate (g/s)
P	pressure (MPa)
q	heat flux (W/m^2)
Q	heating power (W)
T	temperature ($^{\circ}\text{C}$)
U	voltage (V)
x	vapor quality (-)

Greek symbols

ρ	density (kg/m^3)
η	heating efficiency

Subscripts

exp	experimental
s	saturation
w	wall
inlet	channel inlet
i	at i th thermocouple point

boiling (ONB) for the subcooled boiling of R-134a in a horizontal narrow annular duct with gap of (1.0 and 2.0) mm. Piasecka and Poniewski [10] investigated the subcooled nucleation hysteresis in a one-side heated narrow rectangular channel with 1 mm depth, 40 mm width and 360 mm vertical length. The temperature distributions of the heated wall were obtained from liquid crystal thermography. The boiling incipience was recognized as a sudden drop of the wall temperature. Though the boiling incipient and the nucleation hysteresis phenomena has been investigated and reported over two decades [11–13], only a few articles were published in literatures because the tiny wall temperature overshoot could be hardly caught and found by experimental investigation.

Mudawar and Bowers [14] figured the drastically different flow patterns as well as unique CHF trigger mechanisms at low and high mass velocity. The liquid film dryout is the mechanism responsible for the relatively low CHF values associated with saturated boiling in long tubes with low inlet subcooling. High CHF values can occur in the subcooled boiling at high mass velocity flow in a short tube with high inlet subcooling and is commonly referred as DNB. Though there are many famous CHF correlations (such as correlations from Katto and Ohno [15], Shah [16], Qu and Mudawar [17], Wojtan et al. [18], and Zhang et al. [19]) which can well predict the CHF values for conventional size channel and mini/micro channel, the CHF mechanism, especially for subcooled boiling, is not well understood yet. It was proposed in Deng's thesis [20] that the CHF could occur in any one of the flow patterns, and the basic mechanism of CHF could be the same in both the subcooled and saturated boiling regimes. A continuous CHF correlation was obtained for various boiling regimes by a systematic investigation on the effect of major variables on CHF, such as pressure, mass velocity, inlet or outlet quality, and test section geometry.

Visualization investigation on flow boiling of water by Wu and Cheng [21] reported long-period/large-amplitude fluctuations at onset of boiling with two-phase flow and single-phase liquid flow appearing alternatively with time in the microchannels. The phase differences between the fluctuations of pressure drop and mass flux were identified as the reason to sustain the flow instability. The follow up research by Wang and Cheng [22] found that the occurrence of microbubble emission boiling (MEB) can remove high heat flux of 14.41 MW/m^2 at a mass flux of $883.8 \text{ kg/m}^2 \text{ s}$ with only a moderate rise in wall temperature.

In this paper the flow boiling behavior of cyclohexane was investigated in an electrically heated minichannel. It was focused on the onset and departure of flow boiling heat transfer characteristics. The heat transfer deterioration due to the departure of flow boiling includes dryout in the saturation boiling regime and departure of nucleate boiling in the subcooled boiling regime. Cyclohexane was used as a model substance of endothermic

hydrocarbon fuel, whose heat transfer characteristics were investigated by our previous literatures [21–23]. The research on flow boiling of cyclohexane could improve the understanding of relevant behavior of endothermic fuel, which is potential to be used as propellant and coolant in the regeneratively cooled hypersonic vehicles. Some novel findings may be significant for the uncovering of the universe mechanism of heat transfer deterioration for subcooled boiling and saturated boiling.

2. Experimental setup

The flow boiling heat transfer characteristics of cyclohexane were experimentally investigated in an electrically heated horizontal minichannel (heated length L : 360 mm; internal diameter D : 2.0 mm; wall thickness: 0.5 mm). The minichannel with material of nickel alloy GH3128, manufactured by China Iron & Steel Research Institute Group (Beijing, China), can work at wall temperature up to 1000°C . The elemental composition of the GH3128 material is shown in Table 1. The average roughness (R_a) of the test channel inner surface is measured as $0.8 \mu\text{m}$ by 3D measuring Laser Microscope Olympus LEXT OLS4000. The stated purity of the used cyclohexane (from Tianjin Fuchen Chemical Agent) is larger than 99.5 wt.%. The experimental facilities and diagrams of the test section were shown in Fig. 1, and also described in detail in previous literatures [23–25].

The cyclohexane was provided by a constant volume pump (Elite P500 from China) with all the fluid out of the pump flowing through the test channel. Therefore the flow rates for the experiments were directly controlled by the pump. The fluid flow stability of the pump is within $\pm 0.5\%$. A Coriolis mass flow meter with accuracy of $\pm 0.1\%$ at the inlet of test section was used to measure the mass velocity which was controlled at 1.0 g/s ($318 \text{ kg/m}^2 \text{ s}$). Electrical insulator were designed and inserted into the flow passage to isolate the alternate current (AC) electrically heated test section. The electrical current and voltage across the test section were measured to obtain the heating power. The outlet pressure and pressure drop across the test section were measured by Rosemont 3051 transducers. Before the fluid pressure controlled

Table 1
Elemental composition of the GH3128 material.

Element	wt.%	Element	wt.%	Element	wt.%
C	≤ 0.05	Al	0.40–0.80	Ce	≤ 0.050
Cr	19.0–22.0	Ti	0.40–0.80	Mn	≤ 0.50
Ni	$> 55.0\%$	Fe	≤ 2.0	Si	≤ 0.80
W	7.5–9.0	B	≤ 0.005	P	≤ 0.013
Mo	7.5–9.0	Zr	≤ 0.06	S	≤ 0.013

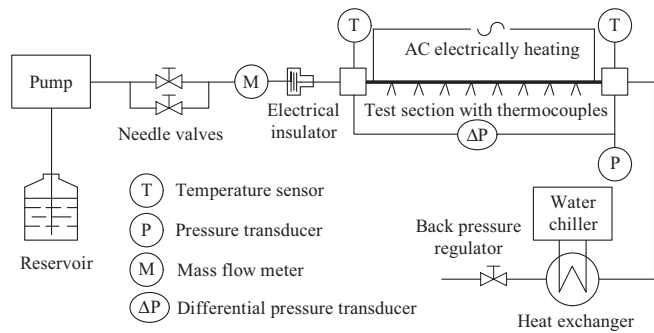


Fig. 1. Schematic diagram of the experimental system.

by a back pressure regulator at the end of the experimental system, the heated fluid out from the test section was cooled by a tubular heat exchanger in which the coolant were from a water chiller.

The fluid inlet and outlet temperatures of the test channel were measured by type K sheathed thermocouples with external diameter of 1.0 mm, which were immersed into working fluid. Some 15 type K thermocouples (TC) with diameter of 0.2 mm were spot-welded on the bottom surface of the test channel with intervals of 25 mm to measure the outside wall temperature. The test minichannel was wrapped by thermal insulation cotton on the outside to reduce heat loss, and also to guarantee the accuracy of wall temperature measurement. All the measured data were put into the computer by Isolated Measurement Pods 3595 (IMP3595 from Solartron Metrology in UK) data acquisition system with frequency of 1 Hz.

3. Data reduction

The local heat flux q was attained by the Eq. (1), in which the heat efficiency η as a function of the channel outside wall temperature was measured by the heat balance method. The Joule heat generated was balanced with the heat loss to the ambience without working fluid employed in the test channel. U and I are the voltage and current through the test channel.

$$q = UI\eta / \pi DL \quad (1)$$

There were some differences amongst the nearly uniform heat fluxes along the test channel, as a result of the differed heat losses which were dependent on the local wall temperatures. However, the discrepancy was less than 5.0% at a wide range of temperature from ambient to 800 °C. The results of the heat efficiency test were calibrated and validated by using an adiabatic channel following the test channel at fluid temperatures from 25 °C to 750 °C. The heating power imposed on the adiabatic channel was indicated as its heat loss while the inlet and outlet fluid temperatures were kept accordant. The electrical resistivity of the material GH3128 of the channels (shown in Table 2) had little effects on the local heat fluxes, because it was almost independent on temperature.

The local fluid enthalpy at the i th TC points h_i was attained by the Eq. (2), where h_{inlet} is the enthalpy of the inlet liquid cyclohexane, and L_i is the distance of the i th TC away from the entrance of the test channel. From the local fluid enthalpy, the local vapor quality (for the saturated liquid–vapor two phase flow) or the fluid temperature (for the subcooled liquid) was calculated.

Table 2
The electrical resistivity ρ of the material GH3128.

$T, ^\circ\text{C}$	17	850	900	950	1000	1050	1100	1150
$\rho, 10^{-6}\Omega \cdot \text{m}$	1.37	1.42	1.39	1.4	1.39	1.38	1.38	1.39

Table 3
Standard uncertainties of the main parameters.

Parameters	Uncertainties (%)
Heat flux q	± 2.2
Mass velocity G	± 3.0
Fluid enthalpy h	± 1.3
Vapor quality x	± 4.0

The thermal properties of cyclohexane (including the vaporization latent and enthalpy) were referred from the NIST REFPROP program.

$$h_i = 1000 \frac{U\eta}{M} \frac{L_i}{L} + h_{\text{inlet}} \quad (2)$$

The inner wall temperature was determined by deducting the calculated temperature drop through the wall [23]. The accuracy of the estimated vapor quality was assured by both the single phase liquid and single phase vapor flow experiments. The standard uncertainties of the parameters were estimated in Table 3. The standard uncertainties of the thermocouples are ± 0.2 °C at temperature $T < 200$ °C, ± 0.5 °C at 200 °C $\leq T < 500$ °C, and ± 1.0 °C at 500 °C $\leq T < 800$ °C.

4. Results and discussion

The heat transfer behavior, especially the subcooled and saturated flow boiling of cyclohexane was experimentally investigated in this study. Some interesting and special heat transfer phenomena are reported and discussed. The subcooled flow boiling and convective heat transfer characteristics of endothermic fuel had been investigated by the literatures of Liu et al. [21–23]. The endothermic fuel is a complicated organic mixture made up of hundreds of components including cycloalkanes, n-alkanes and aromatics. Better understandings of the heat transfer mechanism of endothermic fuel are expected through the investigation of the model pure substance cyclohexane.

4.1. Heat transfer characteristics of cyclohexane

The critical temperature and pressure for cyclohexane are 281 °C and 4.07 MPa respectively from the NIST REFPROP program. As fluid temperature increases, cyclohexane may experience the single phase liquid flow, liquid–vapor two phase flow after the onset of nucleate boiling (ONB), and flow boiling heat transfer deterioration which can occur at subcooled and saturated condition.

As can be seen in Fig. 2, the local wall temperature and heat transfer coefficient profiles of TC7 (in total there were 15 TCs) are showed to demonstrate cyclohexane's heat transfer processes. The bulk fluid temperature T_b increased from room temperature to the saturation temperature T_{sat} of 226.42 °C at $P = 2$ MPa with the increasing heat flux. As to be well known that the nucleation has hysteresis phenomena [10–13], the wall temperature will overshoot a tiny temperature at ONB, which was captured by our study seen in Fig. 2(1) for cyclohexane. At the point of ONB ($T_w = 232.4$ °C, $q = 166.8$ kW/m²) the fluid temperature was less than 100 °C far below the saturation temperature. Before ONB, the wall temperature increased rapidly with the increasing heat flux. After ONB, the wall temperature first decreased to 229.5 °C (at $q = 196.6$ kW/m²) which was indicated as the nucleation hysteresis, and then hardly increased to 231.3 °C (at $q = 480.4$ kW/m²). The wall temperature overshoot measured was 2.9 °C for the nucleation hysteresis here. However, the tiny wall temperature overshoot should not appear or cannot be always observed at ONB, which will be described in detail in the following sections.

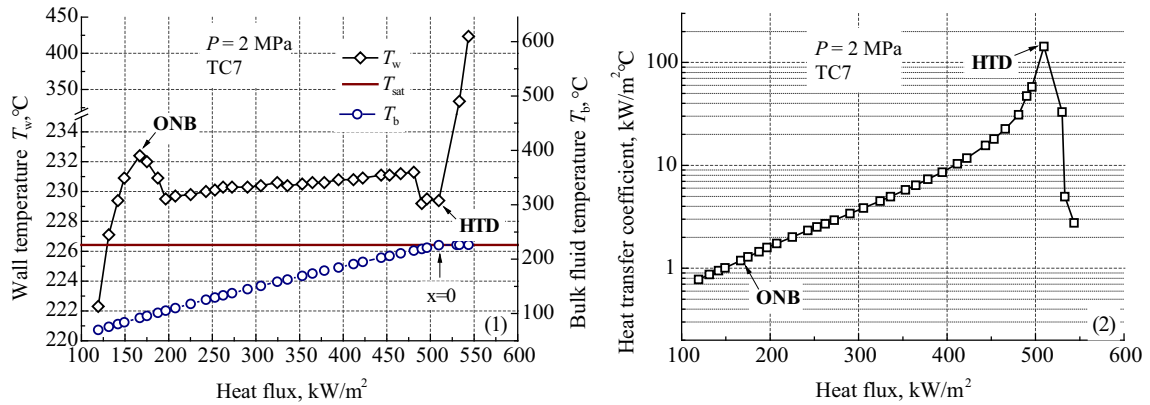


Fig. 2. Heat transfer processes of cyclohexane at subcritical pressure.

In this study we found that the wall temperature experienced a temperature decrease process just before the heat transfer deterioration (HTD), seen in Fig. 2(1). To our best knowledge, the phenomenon is yet unseen and not reported by literatures. Comparison with the wall temperature overshoot at ONB, the wall temperature decrease before HTD had the similar magnitude of 2.1 °C (from 231.3 °C to 229.2 °C). However, comparison with the wall-minus-saturation temperature difference of approximately 5.0 °C, the wall temperature decrease was significant which sharply increased the heat transfer coefficient to above 100 kW/m² °C from 20 kW/m² °C, seen in Fig. 2(2).

The underground mechanism of ONB has been uncovered and widely understood by researchers. Bubble nuclei are formed by vapor trapped in the cavities in the heating surface [26]. During the wall temperature overshoot for the nucleation hysteresis, the start point of temperature drop is regarded as the actual position of the incipient boiling and the bubbles observed move downstream of the heat channel [27]. However, the wall temperature decrease before HTD is difficult to explain.

4.2. Flow boiling heat transfer processes

Flow boiling heat transfer coefficient is always dependent on heat flux. The heat transfer processes at the same fluid condition may be very different according to the heat fluxes. Fig. 3 shows the wall temperature profiles along the test channel at different TC points with different enthalpies for different heat fluxes. Cyclohexane’s saturation temperature is 182.0 °C at P = 1.0 MPa. It can be clearly seen that wall temperatures at different heat fluxes were very closed around $T_w = 200$ °C, which is a result of

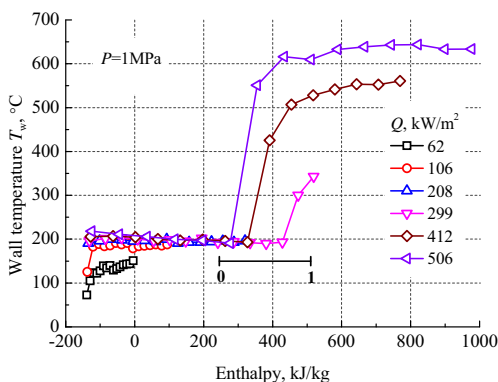


Fig. 3. Wall temperature profiles along the test channel with different fluid enthalpies for different heat fluxes.

the fully developed nucleate boiling (FDB) heat transfer previously described and analyzed in the literature [23] using endothermic fuel as working fluid. The closed temperature distribution indicated that the cyclohexane approached and maintained the FDB condition with the increasing heat fluxes until flow boiling heat transfer deterioration. The fluid temperature or enthalpy varied at different TCs along the test channel and at different heat fluxes. It can be seen that the HTD took place at liquid–vapor two phase flow region with $0 < x$ (vapor quality) < 1.

As can be seen in Fig. 4, the enthalpy of cyclohexane is shown as a function of heat flux for all the TCs along the test channel. The fluid enthalpy increases with the increasing heat flux at the same TC point with the same legend. The flow boiling heat transfer region was represented in the red line enclosed area. The bottom red line is made up of the points of ONB, evaluated by the wall temperature overshoot of nucleation hysteresis. The right red line is made up of the onset points of the HTD for all the TCs.

The vertical dash line for vapor quality $x = 0$ divides the red line enclosed area into the subcooled nucleate boiling area and the saturation flow boiling area. The HTD line locates between the vertical dash line for vapor quality $x = 0$ and $x = 1$, which indicates that the all the HTD occurred in the saturation boiling area. But the HTD points shifted towards the low quality region with the increasing heat flux. At heat flux $q = 500$ kW/m² the HTD point approached zero vapor quality $x = 0$. It can be predicted that subcooled boiling HTD should occur at higher heat fluxes.

The underground mechanism of the HTD may be different while the HTD location forward from high vapor quality (approaching 1) condition to low vapor quality (approaching 0) condition or even subcooled fluid condition, but it cannot be distinguished from

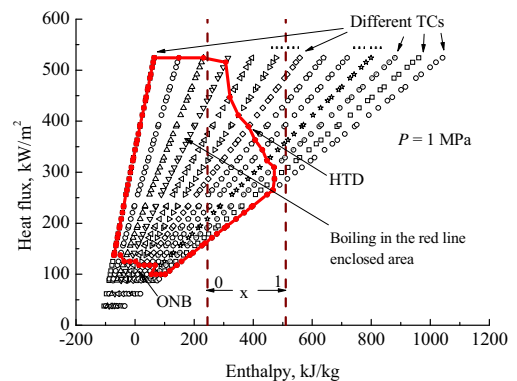


Fig. 4. Flow boiling distribution in the fluid condition map. (For interpretation of the references to colour in this figure legend, the reader is referred to the web version of this article.)

the wall temperature profiles which appeared the same characteristics of sudden rise in wall temperature. At high quality region with low heat flux, dry-out (the second-type HTD) has a more probability to occur. And at the low quality or the subcooled region with high heat flux, the departure of nucleate boiling (DNB) to film boiling (the first-type HTD) has a more probability.

4.3. ONB for cyclohexane

The subcooled flow boiling curves of cyclohexane are showed for different pressures in Fig. 5(1). The wall superheat obtained from TC4 ($L_i/L_h = 105/360$) with heat flux were represented at fluid temperature ranging from 20 °C to approximately 140 °C. It indicated that the flow boiling wall superheat at low pressures are larger than that at high pressures, though the saturation temperature at low pressures is lower, and the heat transfer coefficients are larger at lower pressures, seen in Fig. 5(2). At pressures of (1.0, 2.0, and 3.0) MPa, the wall superheat needed to maintain boiling were (17.5, 7.5 and 1.5) °C respectively.

After ONB, the fully developed boiling (FDB) takes place and the wall temperatures approach a flat area to keep almost no change with the increasing heat flux. However, the wall superheat at FDB conditions can be larger or smaller than that at the ONB point at the relevant pressure. At pressure of 1.0 MPa, the wall temperature continues to increase after ONB. But at pressure of 2.0 MPa, the wall temperatures at FDB conditions do not exceed the values at the ONB point. And at pressure of 3.0 MPa, the temperature overshoot was not observed at ONB.

The wall temperature overshoot in the hysteresis nucleation at pressures of 1.0 MPa and 2.0 MPa can be clearly found in our work, and the profiles of bulk fluid temperature at the ONB points as a function of heat fluxes are shown in Fig. 6. With the same heat flux, bulk fluid temperatures increased along the heated channel. And at the same TC point of the channel the subcooled fluid temperature increased with the increasing heat flux, shown in Fig. 4. At pressures of 1.0 MPa and 2.0 MPa the bulk fluid temperatures at ONB decreased with the increasing heat flux, which is as a result of that the ONB point forwarded to the front of the channel with the increasing heat flux. It can be obviously seen in Fig. 6 that much larger heat fluxes were needed at the higher pressure to trigger the subcooled boiling at the same fluid temperature, though less wall superheat is needed at higher pressure, as shown in Fig. 5(1).

4.4. Wall temperature decrease before HTD

4.4.1. The wall temperature decrease phenomenon (TDP)

In this study we found that there was usually a wall temperature decrease before flow boiling HTD. Fig. 7(1) shows the wall

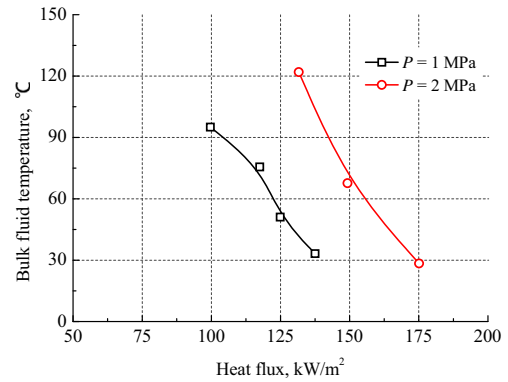


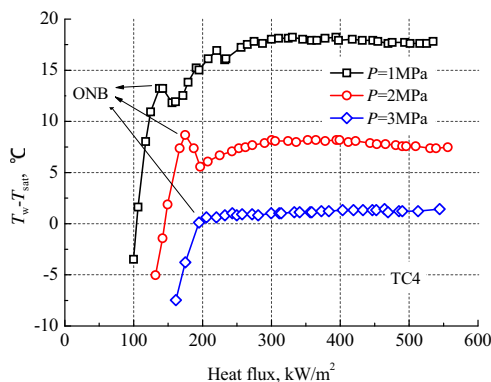
Fig. 6. Bulk fluid temperature at the ONB point for different pressures.

temperature profiles as a function of heat flux for different TCs. It can be clearly seen that the HTD occurred while the wall temperature increased greatly from approximately 200–700 °C. But in the figure the temperature magnitude of the y-axis from 0 to 700 °C is too larger to observe the TDP before HTD. The enlarged y-axis figure is given in Fig. 7(2), the wall temperature decrease of less than 10 °C before HTD can be clearly observed at different heat fluxes for different TCs. As the heat flux increased, the TDP at each TC point maintained in the heat flux interval of at least 50 kW/m² until HTD happened, which proved that the TDP was neither accidental nor transient. The TDP before HTD was an inevitable process at the test conditions.

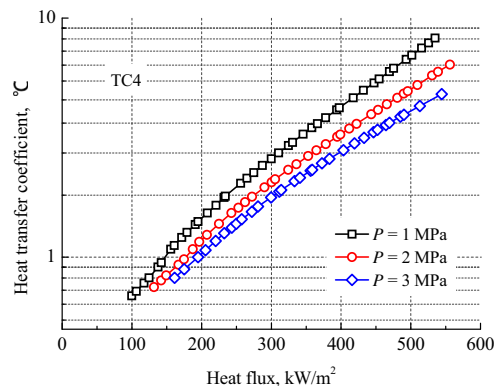
It can be seen in Fig. 7 that during TDP the wall temperature decreases were near 10 °C which were larger than the temperature overshoot (around 3.0 °C) for nucleation hysteresis at ONB. But the temperature decrease during TDP is still a tiny value. Therefore the wall temperature decrease should be confirmed to be not a result of other accidental effects.

First, the TDP was not a result of the electrical resistivity change due to the rising wall temperature. One reason is that the electrical resistivity of the test channel with GH3128 material was not sensitive with the wall temperature, shown in Table 2. Then, even though the resistivity has a small increase with the rising wall temperature at HTD, the electrical resistance of the heater would increase and produce a higher heat flux by imposing a constant current. Additionally, during FDB the wall temperature kept almost no change with heat flux, seen in Figs. 2(1) and 7(2).

Second, the TDP was not a result of the unstable flow. The pressure drop and fluid temperature oscillations were observed after HTD. Fig. 8 shows the pressure drop, bulk fluid temperature and



(1) Wall temperature profiles;



(2) Heat transfer coefficient profiles.

Fig. 5. Subcooled flow boiling curves of cyclohexane at different pressures.

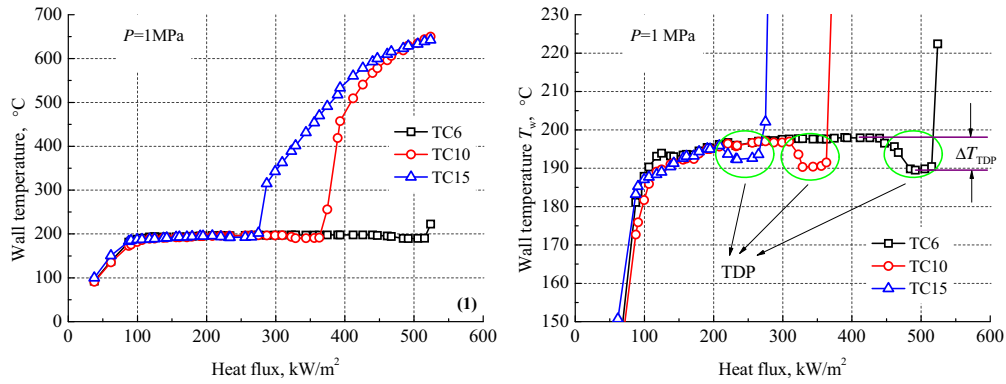


Fig. 7. The wall temperature decrease phenomenon (TDP) before HTD.

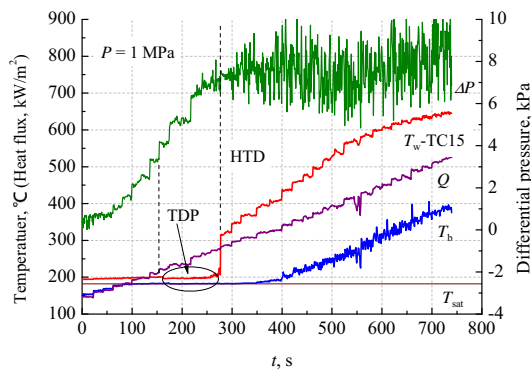


Fig. 8. The oscillations of pressure drop and fluid temperature occur after HTD.

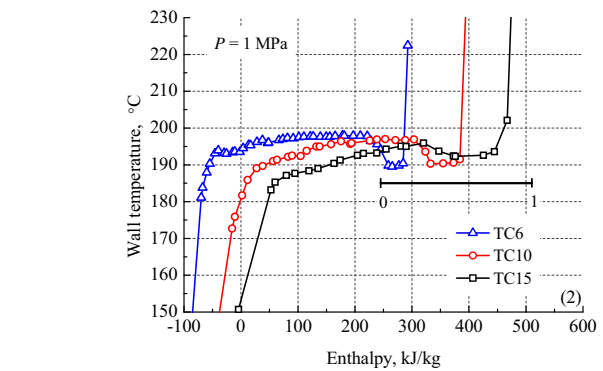


Fig. 9. The wall temperature decrease (TDP) before HTD in wall temperature vs. enthalpy.

wall temperature at TC15 with time as the heat flux increased. It can be seen in Fig. 7 that the HTD occurred at TC15 in the beginning, and then forwards to the front of the test channel with the increasing heat flux. As the HTD occurred at $q = 270 \text{ kW/m}^2$, the pressure drop oscillation started. Though the fluid quality or the fluid temperature continue to increase in the whole test channel, the pressure drop hardly increased at $q = (270 \text{ to } 500) \text{ kW/m}^2$, and the outlet fluid temperature ranging of (182 to 400) °C. But the TDP happened before the beginning of the instability flow. The TDP occurred at $q = 210 \text{ kW/m}^2$ and $\Delta P = 3.0 \text{ kPa}$, there was no pressure drop oscillation during the process of TDP. It indicated that the TDP has no significant effects on the pressure drop oscillation which occurred at the same time with HTD. And also the TDP was proved to be not a result of the unstable flow.

Third, the TDP was not a result of the axial conduction. As heat flux increased, HTD forwarded to the front of the test channel. The TDP coincided to forward. Therefore the TDP can happen at any position of the test channel, which obviously was not related to the axial conduction.

Forth, the TDP was not a result of the passage into the saturation flow boiling from the subcooled boiling. The TDPs are shown in Fig. 9 with wall temperature vs. fluid enthalpy. The TDP occurred at different vapor qualities ranging from 0 to 1. In other words, whatever the HTD is DNB (the first-type HTD) at low quality condition, or dry-out (the second-type HTD) at high quality condition, the TDP would happen. And at TC15, the wall temperature decrease area occupied a wide range of vapor quality from about 0.3 to 0.8. The visible research is needed to uncover the underground HTD mechanism and how the TDP appears.

In the last, the TC temperature measurements were validated and all the TCs were spot-welded on the test channel with good

attachment. Under the alternative current the TC sensors can measure the temperature accurately.

TDP can have a significant role to the prediction of HTD. At HTD condition the wall superheat sharply increases, but the wall temperature experience a decrease process of TDP which enhances the heat transfer performance and gives a signal before the HTD is coming.

4.4.2. Effects of pressure and heat flux on TDP

Pressure has significant effects on the flow boiling heat transfer. As well as the hysteresis nucleation at ONB, the TDP before HTD could also be suppressed by the increasing pressure. Figs. 10 and 11 show the wall temperature vs. fluid enthalpy for different TC

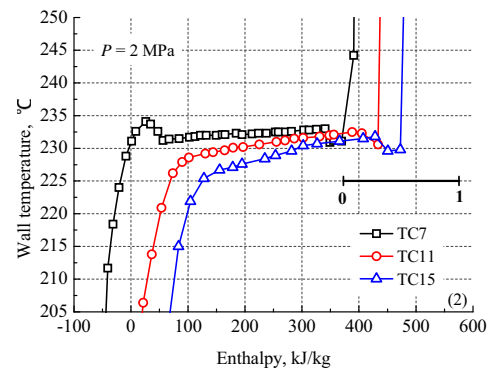


Fig. 10. The wall temperature with fluid enthalpy for different TCs at $P = 2.0 \text{ MPa}$.

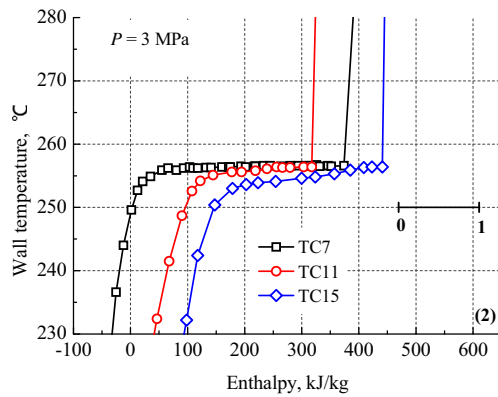


Fig. 11. The wall temperature with fluid enthalpy for different TCs at $P = 3.0$ MPa.

points at $P = 2.0$ and 3.0 MPa. It can be seen that the TDP cannot be observed at $P = 3.0$ MPa. The magnitude of wall temperature decrease during TDP reduced to less than 5°C at 2 MPa from approximately 10°C at 1.0 MPa. However, the TDP can be clearly observed at nearly all the TCs along the test channel at 2.0 MPa.

Celata [13] investigated the hysteresis phenomena in subcooled flow boiling of well-wetting fluids in detail. The wall temperature at boiling inception depends mainly on the pressure while the sub-cooling, mass flux and heat flux seems to be negligible, which also are verified by our results that the wall superheat decreased as the pressure increased, seen in Fig. 5. The nucleation hysteresis also became reduced. The overshoot wall temperatures at ONB were reduced as the pressure increased. Similar to the hysteresis nucleation, the wall temperature decreases during TDP were also suppressed with the increasing pressure.

Effects of heat flux on TDP were investigated. During the fully developed flow boiling processes, the wall temperature kept wildly increasing with the increasing heat flux. And then TDP took place before HTD. The decreased wall temperature for TDP ΔT_{TDP} were defined as the temperature difference between the highest wall temperature during FDB and the lowest wall temperature during TDP, demonstrated in Fig. 7(2). The decreased wall temperature for TDP ΔT_{TDP} as a function of heat flux was showed in Fig. 12 for different pressures. The heat flux for x -axis denoted the heat flux at the lowest wall temperature during TDP. The TDP occurred at heat flux range of (250 to 500) kW/m^2 in 2 mm inside diameter channel at $P = (1$ and $2)$ MPa. ΔT_{TDP} increased with the increasing heat flux at $P = 1$ MPa, but had a decrease trend with the increasing heat flux at $P = 2$ MPa.

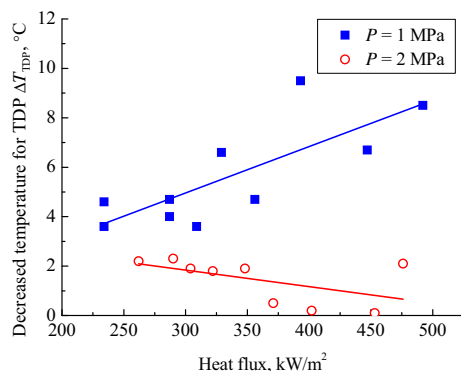


Fig. 12. Variations of the decreased wall temperature for TDP with heat flux for different pressures.

5. Conclusions

The onset of subcooled flow boiling and departure of flow boiling before heat transfer deterioration have been carefully investigated for cyclohexane in a horizontal minichannel in the study. It concluded that:

- (1) The nucleation hysteresis can be clearly observed at onset of nucleate boiling for cyclohexane at pressure of 1.0 and 2.0 MPa, but cannot at 3.0 MPa. Bigger heat flux should be imposed to trigger subcooled boiling at higher pressures. However, both the temperature overshoot due to nucleation hysteresis and wall superheat to maintain boiling conditions decreased with the increasing pressure.
- (2) We experienced a wall temperature decrease phenomenon (TDP) before flow boiling heat transfer deterioration (HTD). The TDP would happen wherever HTD occurred at high quality or low quality conditions. Accompanied with HTD, the TDP can happen at any position of the test channel with different heat fluxes. TDP had a magnitude up to 10.0°C which was larger than the nucleation hysteresis of about 3.0°C for cyclohexane.
- (3) As well as the nucleation hysteresis at ONB, the TDP would be suppressed by the increasing pressure. It can be observed at pressures of 1.0 and 2.0 MPa, but cannot at 3.0 MPa for cyclohexane. Effects of heat flux on TDP were uncertain, for that the decreased wall temperature for TDP increased with the increasing heat flux at pressure of 1 MPa, but had a decrease trend at 2 MPa.

It needs more investigation, such as visible research, for TDP characteristics and to uncover the underground mechanism which may be benefit for the investigation of flow boiling heat transfer deterioration.

Conflict of interest

None declared.

Acknowledgments

This work is sponsored by the National Natural Science Foundation of China (Grant No. 21306147), the National Science Foundation for Post-doctoral Scientists of China (Grant No. 2013M532044) and the Fundamental Research Funds for the Central Universities. Their financial supports are grateful acknowledged.

References

- [1] M.B. Bowers, I. Mudawar, High flux boiling in low flow rate, low pressure drop mini-channel and micro-channel heat sinks, *Int. J. Heat Mass Transfer* 37 (2) (1994) 321–332.
- [2] A.E. Bergles, J.H. Lienhard V, G.E. Kendall, P. Griffith, Boiling and evaporation in small diameter channels, *Heat Transfer Eng.* 24 (1) (2003) 18–40.
- [3] S.G. Kandlikar, Heat transfer characteristics in partial boiling, fully developed boiling, and significant void flow regions of subcooled flow boiling, *J. Heat Transfer ASME* 120 (1998) 395–401.
- [4] S.G. Kandlikar, Fundamental issues related to flow boiling in minichannels and microchannels, *Exp. Therm. Fluid Sci.* 26 (2002) 389–407.
- [5] S.G. Kandlikar, Heat transfer mechanism during flow boiling in microchannels, in: *ASME 2003 1st International Conference on Microchannels and Minichannels*, Rochester, New York, USA, 2003, pp. 33–46.
- [6] S.G. Kandlikar, P. Balasubramanian, An extension of the flow boiling correlation to transition, laminar, and deep laminar flows in minichannels and microchannels, *Heat Transfer Eng.* 25 (3) (2004) 86–93.
- [7] Sung-Min Kim, I. Mudawar, Universal approach to predicting saturated flow boiling heat transfer in mini/micro-channels – part I. Dryout incipience quality, *Int. J. Heat Mass Transfer* 64 (2013) 1226–1238.

- [8] Sung-Min Kim, I. Mudawar, Universal approach to predicting saturated flow boiling heat transfer in mini/micro-channels – part II. Two-phase heat transfer coefficient, *Int. J. Heat Mass Transfer* 64 (2013) 1239–1256.
- [9] Y.M. Lie, T.F. Lin, Subcooled flow boiling heat transfer and associated bubble characteristics of R-134a in a narrow annular duct, *Int. J. Heat Mass Transfer* 49 (13–14) (2006) 2077–2089.
- [10] M. Piasecka, M.E. Poniewski, Hysteresis phenomena at the onset of subcooled nucleate flow boiling in microchannels, *Heat Transfer Eng.* 25 (3) (2004) 44–51.
- [11] H. Brauer, F. Mayinger, Onset of nucleate boiling and hysteresis effects under forced convection and pool boiling, in: *Proceedings of Engineering Foundation Conference on Pool and External Flow Boiling*, Santa Barbara, CA, 1992, pp. 15–36.
- [12] A. Bar-Cohen, Hysteresis phenomena at the onset of nucleate boiling, in: *Proceedings of Engineering Foundation Conference on Pool and External Flow Boiling*, Santa Barbara, CA, 1992, pp. 1–14.
- [13] G.P. Celata, M. Cumo, T. Setaro, Hysteresis phenomena in subcooled flow boiling of well-wetting fluids, *Exp. Heat Transfer* 5 (4) (1992) 253–275.
- [14] I. Mudawar, M.B. Bowers, Ultra-high critical heat flux (CHF) for subcooled water flow boiling—I: CHF data and parametric effects for small diameter tubes, *Int. J. Heat Mass Transfer* 42 (8) (1999) 1405–1428.
- [15] Y. Katto, H. Ohno, An improved version of the generalized correlation of critical heat flux for the forced convective boiling in uniformly heated vertical tubes, *Int. J. Heat Mass Transfer* 27 (9) (1984) 1641–1648.
- [16] M. Shah, Improved general correlation for critical heat flux during upflow in uniformly heated vertical tubes, *Int. J. Heat Fluid Flow* 8 (1987) 326–335.
- [17] W. Qu, I. Mudawar, Measurement and correlation of critical heat flux in two-phase microchannel heat sinks, *Int. J. Heat Mass Transfer* 47 (2004) 2045–2059.
- [18] L. Wojtan, R. Revellin, J.R. Thome, Investigation of saturated critical heat flux in a single uniformly heated microchannel, *Exp. Therm. Fluid Sci.* 30 (2006) 765–774.
- [19] W. Zhang, T. Hibiki, K. Mishima, Y. Mi, Correlation of critical heat flux for flow boiling of water in mini-channels, *Int. J. Heat Mass Transfer* 49 (2006) 1058–1072.
- [20] Z.J. Deng, Prediction of critical heat flux for flow boiling in subcooled and saturated regimes (Ph.D. thesis), Columbia University, UMI, 1998.
- [21] H.Y. Wu, P. Cheng, Visualization and measurements of periodic boiling in silicon microchannels, *Int. J. Heat Mass Transfer* 46 (14) (2003) 2603–2614.
- [22] G. Wang, P. Cheng, Subcooled flow boiling and microbubble emission boiling phenomena in a partially heated microchannel, *Int. J. Heat Mass Transfer* 52 (1) (2009) 79–91.
- [23] Z.H. Liu, Q.C. Bi, Y. Guo, Q.H. Su, Heat transfer characteristics during subcooled flow boiling of a kerosene kind hydrocarbon fuel in a 1 mm diameter channel, *Int. J. Heat Mass Transfer* 55 (19–20) (2012) 4987–4995.
- [24] Z.H. Liu, Q.C. Bi, Y. Guo, J.G. Yan, Z.Q. Yang, Convective heat transfer and pressure drop characteristics of near-critical-pressure hydrocarbon fuel in a mini-channel, *Appl. Therm. Eng.* 51 (2013) 1047–1054.
- [25] Z.H. Liu, Q.C. Bi, Y. Guo, X.S. Ma, Z.Q. Yang, J.G. Jian, S.L. Hu, Hydraulic and thermal effects of coke deposition during pyrolysis of hydrocarbon fuel in a mini-channel, *Energy Fuels* 26 (6) (2012) 3672–3679.
- [26] A.E. Bergles, W.M. Rohsenow, The determination of forced-convection surface boiling heat transfer, *J. Heat Transfer* 86 (1964) 365–372.
- [27] R. Hino, T. Ueda, Studies on heat transfer and flow characteristics subcooled flow boiling – part 1. Boiling characteristics, *Int. J. Multiphase Flow* 11 (3) (1985) 269–281.